The Contribution of Carbon and Water in Modulating Wood Formation in Black Spruce Saplings[1]

Annie Deslauriers, Jian-Guo Huang*, Lorena Balducci, Marilène Beaulieu, and Sergio Rossi

Département des Sciences Fondamentales, Université du Québec à Chicoutimi, Chicoutimi, Quebec, Canada G7H2B1 (A.D., L.B., M.B., S.R.); and Key Laboratory of Vegetation Restoration and Management of Degraded Ecosystems (J.-G.H., S.R.) and Provincial Key Laboratory of Applied Botany (J.-G.H.), South China Botanical Garden, Chinese Academy of Sciences, Guangzhou 510650, China

ORCID IDs: 0000-0003-3830-0415 (J.-G.H.); 0000-0001-5248-9096 (M.B.).

Nonstructural carbohydrates (NSCs) play a crucial role in xylem formation and represent, with water, the main constraint to plant growth. We assessed the relationships between xylogenesis and NSCs in order to (1) verify the variance explained by NSCs and (2) determine the influence of intrinsic (tissue supplying carbon) and extrinsic (water availability and temperature) factors. During 2 years, wood formation was monitored in saplings of black spruce (*Picea mariana*) subjected to a dry period of about 1 month in June and exposed to different temperature treatments in a greenhouse. In parallel, NSC concentrations were determined by extracting the sugar compounds from two tissues (cambium and inner xylem), both potentially supplying carbon for wood formation. A mixed-effect model was used to assess and quantify the potential relationships. Total xylem cells, illustrating meristematic activity, were modeled as a function of water, sucrose, and D-pinitol (conditional r^2 of 0.79). Water availability was ranked as the most important factor explaining total xylem cell production, while the contribution of carbon was lower. Cambium stopped dividing under water deficit, probably to limit the number of cells remaining in differentiation without an adequate amount of water. By contrast, carbon factors were ranked as most important in explaining the variation in living cells (conditional r^2 of 0.49), highlighting the functional needs during xylem development, followed by the tissue supplying the NSCs (cambium) and water availability. This study precisely demonstrates the role of carbon and water in structural growth expressed as meristematic activity and tissue formation.

Mobile sugars (e.g. Suc, Glc, and Fru) and sugar alcohols (e.g. pinitol) play an essential role in sustaining plant growth and metabolism and plant signaling (Muller et al., 2011). The origin of nonstructural carbohydrates (NSCs; reserve versus recent photosynthetic products) and their importance for growth processes are currently under intensive investigation (Wiley and Helliker, 2012; Rocha, 2013). Carbon (C) incorporation during wood formation, mostly in the form of cellulose and other cell wall polymers, determines most of the biomass accumulated by trees. In red maple (*Acer rubrum*), the NSC used to build the xylem is less than 1 year old (Carbone et al., 2013), demonstrating a fast incorporation of C originating from the mobile sugar pool in the stem. Reserves often are used at growth resumption in early spring (Oribe et al., 2003; Begum et al., 2013), but most xylem is formed with newly synthesized NSCs (Hansen and Beck, 1990, 1994; Kagawa et al., 2006). The ray parenchyma cells in xylem also could act as a source of NSCs to sustain growth when assimilates coming from the leaf become scarce (Maunoury-Danger et al., 2010; Olano et al., 2013), such as during a water deficit. As the molecular networks driving cell division and expansion largely rely on the availability of carbohydrates to provide energy and biomass (Lastdrager et al., 2014), xylem formation is an ideal system in which to study source-sink relationships and the C dependence of growth metabolism.

The cambium is the meristem that produces layers of phloem and xylem cells in stem, branches, and roots with a periodic activity that results in seasonal radial growth (Rossi et al., 2013). The machinery of growth requires C resources for many processes, in particular to supply energy for division, generate water turgor pressure during cell expansion, and produce polysaccharides during cell wall formation (Muller et al., 2011). Recent evidence strongly supports the association between the pattern of NSCs and wood formation: the rate of xylem growth follows the concentration of NSCs in cambium, reflecting the strong demand for C

[1] This work was supported by the Natural Sciences and Engineering Research Council of Canada (discovery grant to A.D.), by Mitacs (grant to J.-G.H. and the Consortium de Recherche sur la Forêt Boréale Commerciale), by the 100 Talents Program of the Chinese Academy of Sciences (grant no. Y421081001 to J.-G.H.), and by the National Natural Science Foundation of China (grant no. 31570584 to J.-G.H.).

* Address correspondence to huangjg@scbg.ac.cn.

The author responsible for distribution of materials integral to the findings presented in this article in accordance with the policy described in the Instructions for Authors (www.plantphysiol.org) is: Annie Deslauriers (adeslaur@uqac.ca).

A.D. and S.R. elaborated the concept behind the experiment; A.D. wrote the article with the help of the other authors; J.-G.H. elaborated and realized the mixed-model effect; M.B. and L.B. performed the sampling and the NSC and wood formation analyses, respectively.

www.plantphysiol.org/cgi/doi/10.1104/pp.15.01525

compounds in the phases of cell enlargement and cell wall thickening (Deslauriers et al., 2009; Simard et al., 2013). Specific C compounds are needed according to the stage of wood development: increases in volume during cell expansion (i.e. cell growth) need osmotically active C compounds and water to generate a suitable wall-yielding turgor pressure in growing cells (Steppe et al., 2015), while cell maturation needs C compounds as a substrate to build cell walls (Koch, 2004). The mobile pool of sugars allocated to growing and differentiating cells thus represents a direct constraint to wood formation (Michelot et al., 2012; Simard et al., 2013). Two nearby mobile carbohydrate pools can directly sustain wood formation: cambium, assuming that the C compound comes from Suc unloaded from phloem; and xylem, assuming that the C compound comes from ray parenchyma (Deslauriers et al., 2009; Giovannelli et al., 2011). Therefore, a relationship between the forming xylem and the available soluble sugars in each pool could significantly improve our understanding of the use of NSCs in secondary growth and the importance of their provenance (current photosynthesis versus reserve). Compared with the outermost xylem, much higher amounts of NSCs are found in cambium (Deslauriers et al., 2009; Simard et al., 2013) because of its proximity to the unloading sites in phloem.

In the absence of water deficit, correlations are reported between the growth of various organs and C availability (in roots, young leaves, flowers, fruits, and seeds), but these relationships can be modified or reduced under stress (for review, see Muller et al., 2011; Tardieu et al., 2011). Drought-related growth reductions are caused primarily by hydromechanical constraints rather than C availability (Pantin et al., 2013; Steppe et al., 2015), which could explain the uncoupling between NSCs and cell growth. Therefore, characterization of the interacting role of C and water availability in xylem cell differentiation is needed, as well as the main source of C for wood formation.

The objectives of this study were (1) to verify the relationships between xylem production and available NSCs and (2) to determine the influence of tissue supplying NSCs, water availability, and temperature in black spruce (*Picea mariana*). In the study, xylem production was characterized by the living cells (the sum of the number of cells in cambium, enlargement, and cell wall thickening), representing the cells with high metabolic activity, and by the total number of xylem cells formed (differentiating and mature cells), representing the sum of tree-ring growth during the growing season (Fig. 1). The tissue supplying C represents the NSCs coming from cambium or the inner xylem (Fig. 1). In relation to the objectives, we considered the following hypotheses: the amount of available NSCs located in cambium or xylem sustains the metabolic activity of the living cells and influences the total number of cells produced; and intrinsic (tissue preferentially supplying C) and extrinsic (water availability and temperature) factors represent constraints to NSC availability and xylem production.

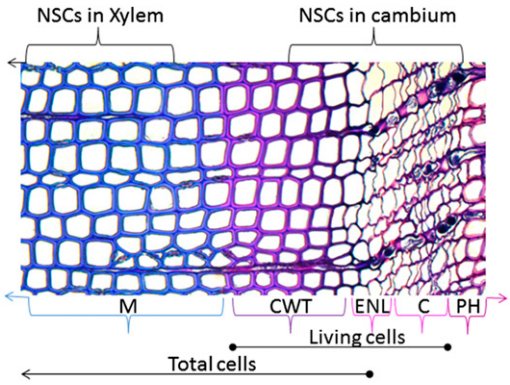

Figure 1. Differentiating cells during wood formation (C, cambium; CWT, cell wall thickening; ENL, enlargement) and the mature cell (M). The living cells in the analyses included cambium, enlargement, and cell wall thickening, while the total cell represents enlargement, cell wall thickening, and mature cells. The available NSCs were measured in the cambium and xylem. PH, Living phloem.

RESULTS

Tree Growth

Radial growth of the irrigated saplings showed a typical S-shaped curve for all temperature treatments (total cells; Fig. 2). The increase in cell number was similar in nonirrigated and irrigated saplings before the treatment. At the end of the water deficit, the increase in total cells was observed to slow down or stop for several weeks in nonirrigated saplings, while growth continued undisturbed in irrigated saplings. On days of the year (DOY) 200 to 220, a new sharp increase in radial growth was observed in nonirrigated saplings, although the total cell number always remained lower than in irrigated saplings until the end of the growing season.

With respect to radial growth (i.e. the increase in xylem cells), apical growth occurred quickly, with the maximum length being reached in 15 to 20 d (Fig. 2). In both study years, this sharp increase was synchronous between the different treatments and started when irrigation was withheld. After the maximum apical length was reached, the observed deviations were caused by sapling difference in height growth, which was higher in 2011 compared with 2010.

Similar annual trends of living cells were observed between the temperature and water treatments (Fig. 2). The living cells were characterized by bell-shaped curves, with a depression at about one-third of the growing season for both water and temperature treatments. In May 2010, cambium division and cell enlargement had already started, as indicated by a number of cells varying between 10 and 20, depending on the temperature treatment (Fig. 2). In May 2011 (around

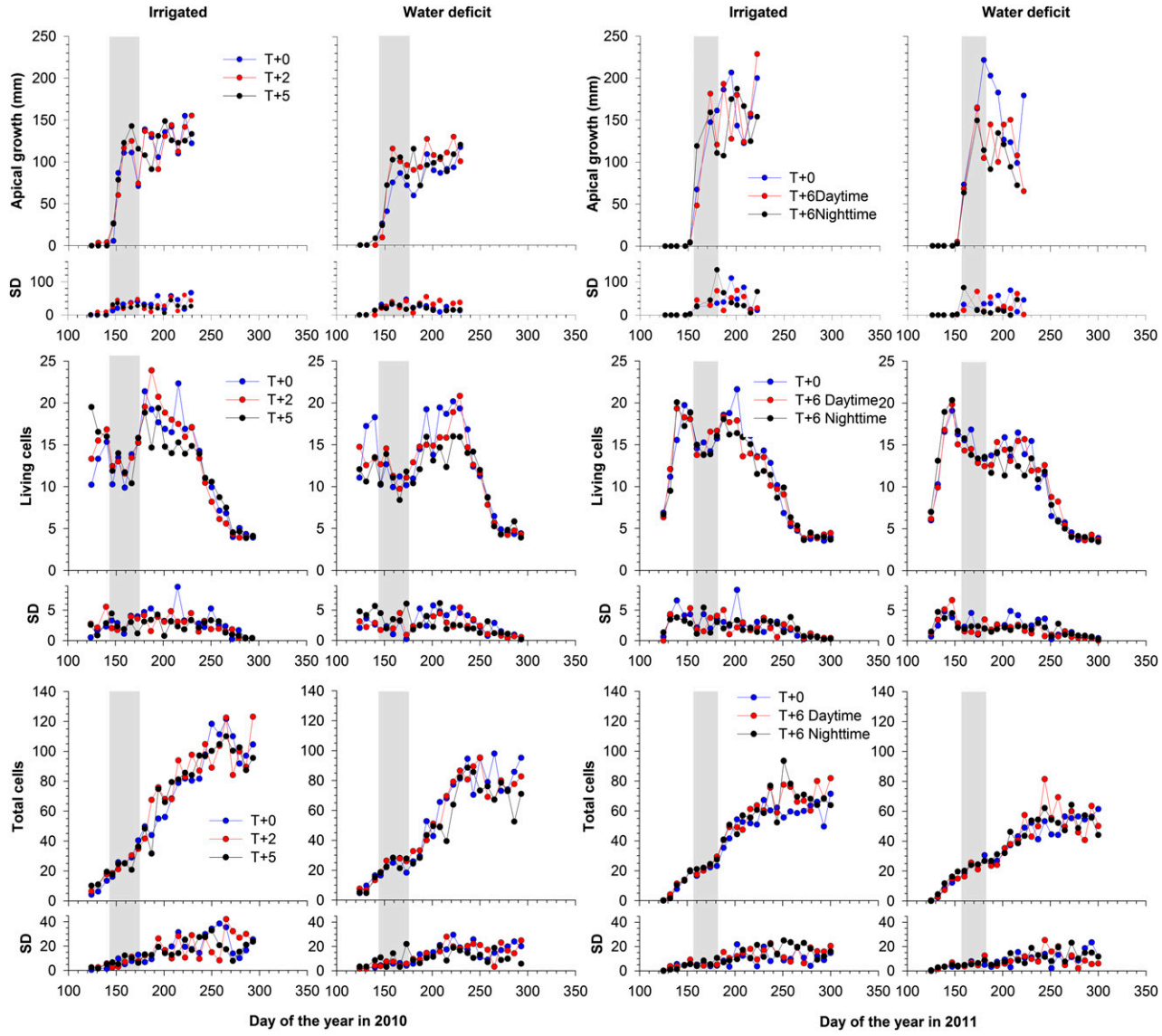

Figure 2. Dynamics of wood formation in 2010 (left) and 2011 (right) represented as mean values. The living cell represents the sum of cambial cells, cells in enlargement, and cells in wall formation. The total cell represents tree-ring growth as the sum of cells in enlargement, cells in wall formation, and mature cells. In 2010, the temperature treatments were T+0 (blue lines), T+2 (red lines), and T+5 (black lines). In 2011, the temperature treatments were T+0 (blue lines), T+6 daytime (red lines), and T+6 nighttime (black lines). The gray bands indicate the periods when irrigation was withheld. SD indicates standard deviation among the measured values in the corresponding graph.

DOY 120), only the cambium was already active, with six to seven cells on average but no cell differentiation. Around DOY 160 to 170, the number of living cells decreased to a minimum of nine to 10 and 12 to 15 in 2010 and 2011, respectively. These drops in living cells were synchronized with the start of the apical growth of the saplings (Fig. 2). After this drop, the number of living cells increased rapidly to its maximum, while the increase was much slower in saplings subjected to water deficit. Once annual activity had ended and the cambium stopped dividing, the number of living cells decreased gradually to the minimum value, corresponding to quiescence conditions of the cambium meristem. Between four and six cambial cells were observed in autumn, fewer than at the beginning of the season (Fig. 2).

Correlations among NSCs

In cambium of irrigated saplings, the variation of Suc was correlated mainly with D-pinitol (r = 0.53) and marginally with raffinose (r = 0.30) and Fru (r = 0.23; Table I). Fru varied according to Glc, with a correlation coefficient of 0.88. Fru was marginally correlated with D-pinitol (r = 0.31). In xylem of irrigated samplings, the correlations between the soluble sugars were slightly different. Suc was correlated with raffinose (r = 0.36)

Table I. *Pearson correlation coefficients between NSCs*

In irrigated sampling (left part), the correlations were performed between the soluble sugars measured in cambium (bold; $n = 188$) and xylem ($n = 223$). In water deficit sampling (right part), the correlations were performed between the soluble sugars measured in cambium (bold; $n = 163$) and xylem ($n = 215$). Asterisks indicate significant correlation coefficients: ***, $P < 0.0001$; **, $P < 0.001$; and *, $P < 0.05$. D-Pin, D-Pinitol; Raf, raffinose.

	Irrigated					Water Deficit				
	Suc	D-Pin	Fru	Glc	Raf	Suc	D-Pin	Fru	Glc	Raf
Suc		**0.53*** **	**0.23***	**0.02**	**0.30*** **		**0.54*** **	**0.21***	**0.04**	**0.08**
D-Pin	0.20**		**0.31*** **	**0.05**	**0.08**	0.15*		**0.28****	**0.12**	**0.23***
Fru	−0.08	0.71***		**0.88*** **	**0.28*** **	−0.22**	0.57***		**0.89*** **	**0.08**
Glc	−0.15*	0.65***	0.98***		**0.17***	−0.28***	0.46***	0.97***		**0.00**
Raf	0.36***	0.09	0.25***	0.26***		0.27***	0.09	0.04	0.02	

but not with D-pinitol (Table I). The variation of D-pinitol in the xylem was positively correlated with Glc ($r = 0.65$) and Fru ($r = 0.71$; Table I). As for cambium, the variation of Fru and Glc in xylem was highly similar ($r = 0.98$).

In general, the correlations between the soluble sugars were mostly similar in saplings subjected to water deficit. In cambium, Suc was correlated with D-pinitol ($r = 0.54$) and Fru ($r = 0.21$) but not with raffinose. However, D-pinitol and raffinose showed a positive correlation ($r = 0.23$). Suc was negatively correlated with Fru and Glc, as shown by the correlation coefficients of −0.22 and −0.28, respectively.

Variation in NSCs

NSCs measured in cambium or xylem had similar trends irrespective of the treatments (Fig. 3). Therefore, the means represent all temperature treatments confounded (for full NSC time series and statistical analyses, see Deslauriers et al., 2014). In cambium, Suc was up to 30 times more abundant than the other NSCs (Fig. 3), followed by D-pinitol and Fru. In both years, the withholding of irrigation caused a small decrease in Suc and Fru and a sharp increase in raffinose observed around the end of the water deficit period (Fig. 4). Although the concentrations of NSCs were much lower in the inner xylem, trends analogous to that of cambium were observed in xylem.

Parallel variations were observed between NSCs and the number of living cells (Figs. 2 and 3). When cambial activity started, between DOY 120 and 130, the amount of NSCs in cambium was high. A decline was observed between DOY 150 and 170, which was more pronounced in 2010, with concentrations close to zero. A second decline was observed in mid-July (DOY 208 in 2010 and DOY 196 in 2011).

Mixed-Effects Model

The results from the null models (total and living cells) showed that random effects were significant, particularly at the tree level with high intraclass correlation (Table II). Therefore, the random effects were included in the mixed-effects model. Random slopes and interactive effects of temperature × water treatments were not

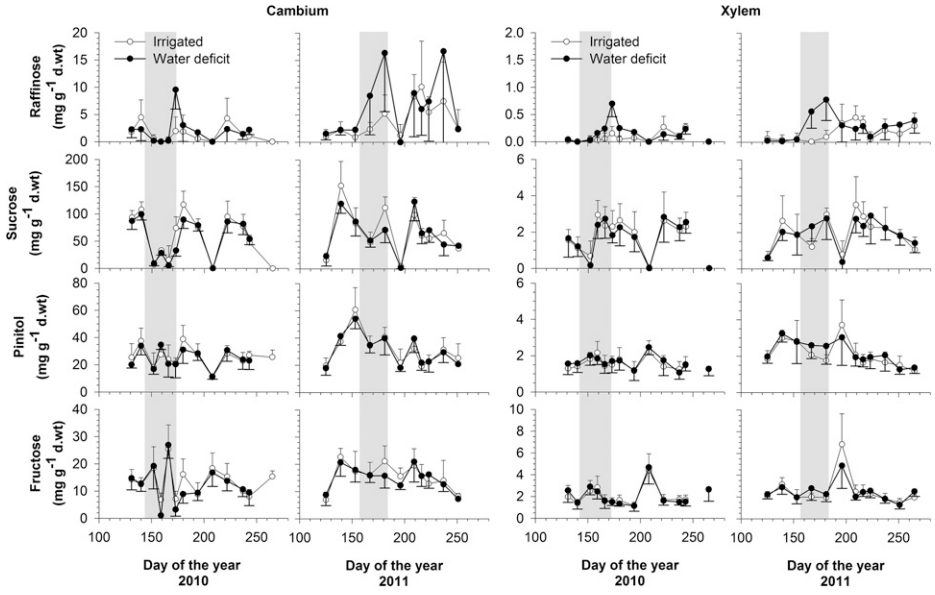

Figure 3. Mean soluble sugars in cambium and xylem measured during 2010 and 2011.The vertical bars represent the SD among the measured trees (all temperature treatments confounded). White circles represent the irrigated plants, and black circles represent water deficit plants. The gray bands indicate the periods when irrigation was withheld. Note the different ranges of the vertical axes between cambium and xylem. d.wt, Dry weight.

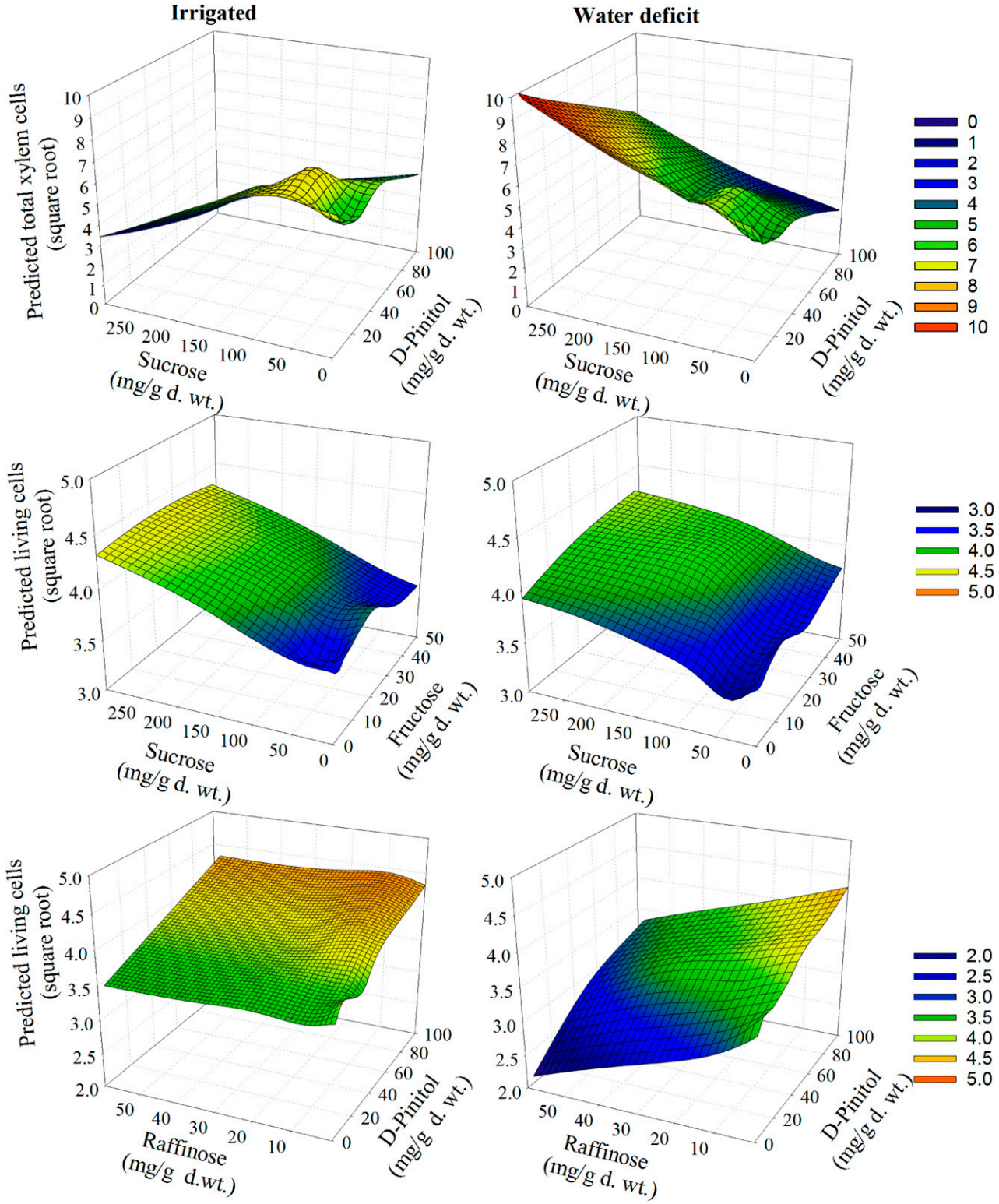

Figure 4. Surface plot (after smoothed spline interpolation based on $n = 3{,}348$ for irrigated and $n = 2{,}937$ for water deficit). The relationships are illustrated between the predicted total xylem cells (square root) and Suc and D-pinitol (top) and between the predicted living cells (square root) and Suc and Fru (middle) and raffinose and D-pinitol (bottom). The unit for Suc, D-pinitol, Fru, and raffinose is mg g^{-1} dry weight (d.wt.).

significant and so were excluded from the final model. A full model was built and considered the best model for total xylem cells and living cells in terms of minimum AIC, AICC, and BIC. The good performance of the two full models is also reflected by their high conditional r^2 (over 0.79 for total cells and 0.49 for living cells).

We found that the increase in the number of total xylem cells during the growing season can be modeled as a function of Suc, D-pinitol, and water treatments as well as random effects. For the other model, the living cells can be modeled as a function of raffinose, Suc, D-pinitol, Fru, the tissue where the sugars were extracted, water and temperature treatments, as well as random effects. Even if significant, fixed effects only accounted for a small portion of variance, as shown by the lower proportion change in variance (Table II) and marginal r^2 (Table III). The majority of the variance was explained by the random effects, as indicated by the lower proportion change in variance and the large difference between the marginal and conditional r^2 (Table III). This could be explained by the high variance in the measured cell numbers, especially for the total xylem cells (Fig. 2). Nevertheless, the number of total xylem cells and living cells changed positively or negatively according to the water treatment and specific sugar compounds (Fig. 4).

Both full models demonstrated that the water treatment was a significant variable to account for the variations in cell number, particularly for the predicted total xylem cells ($P < 0.0001$; Table II) compared with living cells ($P < 0.05$; Table II). In general, we found the decline in the variance of total xylem cells and living cells explained under the water deficit treatment compared with the irrigated treatment, as shown by the marginal r^2 when tissue and temperature were fixed (Table III).

In terms of difference among temperature treatments, most of the temperature treatments were not significant (Table II). Therefore, temperature did not influence the variations in total xylem cells and slightly explained the variation in the living cells ($P < 0.05$ for the T+2 treatment only [for definitions, see "Materials and Methods"]). The variance of total xylem cells and living cells explained under the different thermal treatments was generally higher in T0, T+6 daytime, and T+6 nighttime compared with T+2 and T+5, as shown by the marginal r^2 (Table III). Compared with 2011, higher temperatures were registered in 2010, mainly due to a warmer spring (Fig. 5), with the greenhouse conditions being above the long-term average calculated for the boreal stands.

The decomposition of variance (DOV) also precisely indicated the contribution of each fixed effect to both

Table II. *Statistics of the null and full models built for the predicted total xylem cells (left) and living cells (right)*

SE is reported in parentheses; ***, $P < 0.0001$; **, $P < 0.001$; and *, $P < 0.05$. ICC, Intraclass correlation; PCV, proportion change in variance; AIC, Akaike's information criterion; AICC, corrected Akaike's information criterion; BIC, Sawa Bayesian information criterion.

Dependent Variables	Total Xylem Cells		Living Cells	
	Null Model ($\times 10^{-2}$)	Full Model ($\times 10^{-2}$)	Null Model ($\times 10^{-2}$)	Full Model ($\times 10^{-2}$)
N	6,357	6,264	6,360	6,267
Fixed effects				
Intercept (β_0)	591.61 (8.74)***	620.00 (28.18)***	368.17 (1.90)***	331.43 (7.50)***
Raffinose (β_1)		−0.21 (1.42)		−1.45 (0.43)***
Suc (β_2)		0.47 (0.20)*		0.27 (0.06)***
D-Pinitol (β_3)		−1.85 (0.51)***		0.51 (0.19)**
Fru (β_4)		−0.02 (1.13)		1.35 (0.36)***
Tissue (xylem, β_5 versus cambium)		6.52 (23.86)		28.27(6.42)***
Temperature (warm versus T+0)				
Temperature (T+2; β_6)		45.86 (25.78)		12.02 (5.40)*
Temperature (T+5; β_6)		34.79 (25.72)		7.20 (5.42)
Temperature (T+6 daytime; β_6)		−11.04 (25.70)		1.82 (5.44)
Temperature (T+6 nighttime; β_6)		−24.03 (25.66)		−0.34 (5.46)
Water (water deficit; β_7 versus irrigated)		−70.26 (17.06)***		−11.06 (3.62)*
Random effects				
Residuals (additive dispersion)	111.81 (2.41)***	108.98 (2.37)***	24.11 (0.60)***	23.94 (0.59)***
Tree (tissue × temperature × water)	528.91 (29.18)***	493.02 (27.66)***	20.42 (1.44)***	17.57 (1.28)***
Repeated measurement (tree)	21.63 (1.48)***	21.18 (1.50)***	31.53 (1.58)***	30.69 (1.58)***
ICC (measurements)	3.27%		41.45%	
ICC (tree)	79.85%		26.85%	
PCV (measurements)		2.08%		2.66%
PCV (tree)		6.79%		13.96%
PCV (residuals)		2.53%		0.71%
Model fit				
−2 log likelihood	2,0871.7	2,0395.4	9,556.1	9,335.1
AIC	2,0879.7	2,0423.4	9,564.1	9,363.1
AICC	2,0879.7	2,0423.4	9,564.1	9,363.2
BIC	2,0871.7	2,0395.4	9,556.1	9,335.1

Table III. *Marginal and conditional r^2 explained by the full model for total xylem cells and living cells under different treatments*

The treatments are expressed as the combination of tissue (xylem versus cambium), water treatment (irrigated versus water deficit), and temperature treatment (T+0 versus T+2, T+5, T+6 daytime, and T+6 nighttime). Values shown are percentages.

Treatment Combinations	Total Xylem Cells		Living Cells	
	Marginal r^2	Conditional r^2	Marginal r^2	Conditional r^2
Cambium, irrigated				
T+0	1.20	79.58	4.79	52.06
T+2	0.27	79.39	2.66	50.99
T+5	2.07	79.76	2.91	51.11
T+6 daytime	1.02	79.54	3.63	51.48
T+6 nighttime	1.55	79.65	4.79	52.06
Cambium, water deficit				
T+0	0.82	79.50	4.34	51.83
T+2	2.81	79.91	2.57	50.94
T+5	0.84	79.50	2.62	50.97
T+6 daytime	0.94	79.52	4.06	51.69
T+6 nighttime	0.68	79.47	4.34	51.83
Xylem, irrigated				
T+0	1.10	79.56	0.85	50.08
T+2	0.25	79.38	0.20	49.75
T+5	0.44	79.42	0.19	49.75
T+6 daytime	0.17	79.37	0.06	49.68
T+6 nighttime	1.01	79.54	0.85	50.08
Xylem, water deficit				
T+0	0.03	79.34	0.48	49.90
T+2	0.43	79.42	0.06	49.68
T+5	0.03	79.34	0.10	49.70
T+6 daytime	0.61	79.46	0.05	49.68
T+6 nighttime	0.44	79.42	0.48	49.89

dependent variables (Fig. 6). The DOV indicated that water availability was a crucial factor influencing the total number of xylem cells (73%), while Suc (23%) and tissue (23%) were both most influential in predicting the number of living cells. Of the NSC concentrations, D-pinitol (10.5%) and Suc (7.9%) were significantly related to the total xylem cells, while all the C variables (Suc, Fru, raffinose, and D-pinitol, accounting for 59% in total) were, in turn, significantly associated with living cells (Fig. 6). The tissue was found to be a significant variable explaining the predicted living cells, as suggested by a higher percentage of DOV. Interestingly, more variance in the predicted living cells can be accounted for by the NSCs extracted from cambium than xylem, as indicated by higher marginal r^2 for cambium under constant water and temperature treatments (Table III). However, the variable tissue was not significant for the predicted total xylem cells, as shown by a lower percentage of DOV (0.14%) and the more or less similar variance explained between cambium and xylem when under the same water and temperature treatments (Table II).

DISCUSSION

In this study, xylogenesis was modeled as a function of NSC availability and other intrinsic (tissue) and extrinsic (water availability and temperature) factors. Similar variations between xylogenesis and NSCs also were observed in conifers (larch and spruce; Simard et al., 2013) and broadleaves (poplar; Deslauriers et al., 2009). However, to our knowledge, this is the first time that the relationship has been quantified mathematically. We found that the NSCs measured in the cambium zone were more important in explaining the variation in the number of living cells during the growing season. This indicates the preference of mobile sugars probably coming from the recently fixed C unloaded from phloem transport for the metabolic needs of growth. In general, the variance explained in wood formation decreases slightly under water deficit, implying some uncoupling between NSCs and growth, while the warming had very few significant effects.

The Role of Available C during Xylogenesis

Given that wood formation was disentangled in total xylem and living cells, we were able to elucidate the physiological mechanisms underlying the contribution of each NSC variable and water with both models (Figs. 4, 6–7). For living cells (all metabolically active), all the sugar compounds were found to explain their variation, with higher DOV for Suc (22.66%) and Fru (16.76%), followed by raffinose (13.19%) and D-pinitol (6.7%). The most important NSCs explaining the total xylem cells

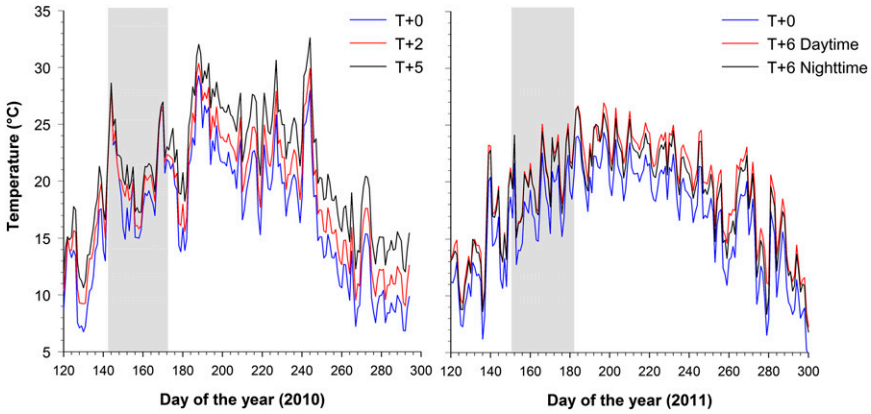

Figure 5. Temperature measured during the experiments in 2010 (left) and 2011 (right). In 2010, the temperature treatments were T+0 (blue line), T+2 (red line), and T+5 (black line). In 2011, the temperature treatments were T+0 (blue line), T+6 daytime (red line), and T+6 nighttime (black line). The gray bands represent the periods when irrigation was withheld during both years.

were Suc (7.88%) and D-pinitol (10.43%) only, as nonliving cells were included in the total xylem cells to account for the entire tree-ring development over time (Fig. 7).

Suc was the main compound forming the NSC pool in cambium (Fig. 2; Deslauriers et al., 2014). This sugar is mainly broken down by invertase, forming hexose (Glc and Fru), and by Suc synthase, forming Fru and UDP-Glc (Koch, 2004). Large concentration gradients of Suc and hexose can be observed between meristematic (high-Suc) and differentiation (high-hexose) zones in root tips (Scheible et al., 1997; Freixes et al., 2002). Even though no spatial gradient of carbohydrate was measured in this study, the amounts of both total xylem (meristematic activity) and living cells (metabolic activity) were positively coupled with Suc. Suc was the most important C compound influencing the variability observed in living cells (Fig. 4, middle), probably because these were composed of a large number of tracheids undertaking secondary cell wall formation (Deslauriers et al., 2014). Indeed, a large quantity of UDP-Glc is required during the process of wall formation

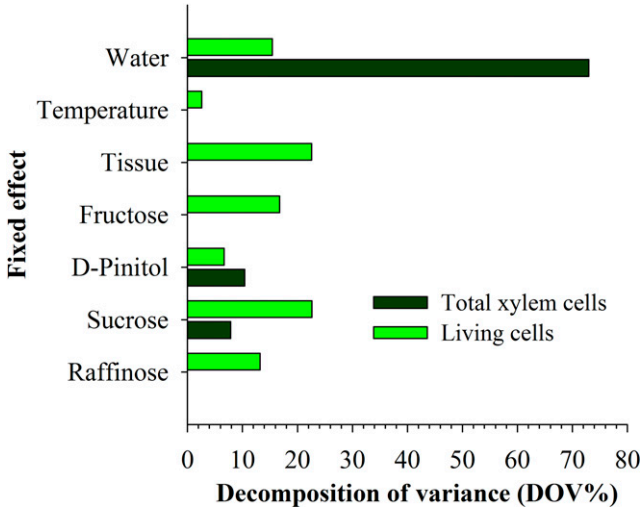

Figure 6. Mixed-model DOV (%) in predicting total xylem cells (dark green) and living cells (light green).

(cell wall thickening; Fig. 1), as the number of cells in this phase represents an irreversible sink for building the material composing the cell walls (cellulose, hemicellulose, and lignin), a process that lasts several weeks in conifers (Deslauriers et al., 2003; Gruber et al., 2010; Cuny et al., 2014).

Moreover, the amount of living cells was explained by Fru (16.76%). As Glc was highly correlated with Fru (correlation coefficient varying between 0.88 and 0.98), the contribution and role of this sugar is expected to be similar to that of Fru. These results are in line with the findings of Freixes et al. (2002), who found a positive correlation between root elongation and hexose concentration in Arabidopsis. The hexose concentration is a good proxy for rapid expansion (Muller et al., 2011). A large amount of hexose is produced from vacuolar invertase to increase cell osmotic potential and generate the appropriate turgor pressure for cell expansion (Koch, 2004). Fru also can be used for ATP production (Koch, 2004), necessary for cell metabolism during the growth processes or active transport of several compounds across membranes. The results for Fru, therefore, support the fact that sugar allocation and partition also could be linked with respiratory processes, as the number of cambium and differentiating cells are related to CO_2 emitted by the stem during wood formation (Lavigne et al., 2004; Gruber et al., 2009).

The osmotically active sugars, D-pinitol and raffinose, also were significant. D-Pinitol explained both total xylem (DOV of 10.43) and living cells (DOV of 6.7), but with a negative and positive influence, respectively (Fig. 5, top). Cyclitols, such as D-pinitol, are normally implicated in cell osmoregulation in order to maintain cell turgor in the case of stress (i.e. cold, drought, or salinity; for review, see Orthen et al., 1994), which could explain the negative influence of this sugar on the total xylem cell, especially under water deficit. However, it cannot be excluded that D-pinitol also might contribute to the overall water potential (maintaining turgor; Orthen et al., 1994; Johnson et al., 1996) and explain the positive influence on the living cells (Fig. 4, bottom). The growing cells first accumulate D-pinitol and hexose in order to regulate cell osmosis to generate the turgor to enlarge and then shift to more complex sugars

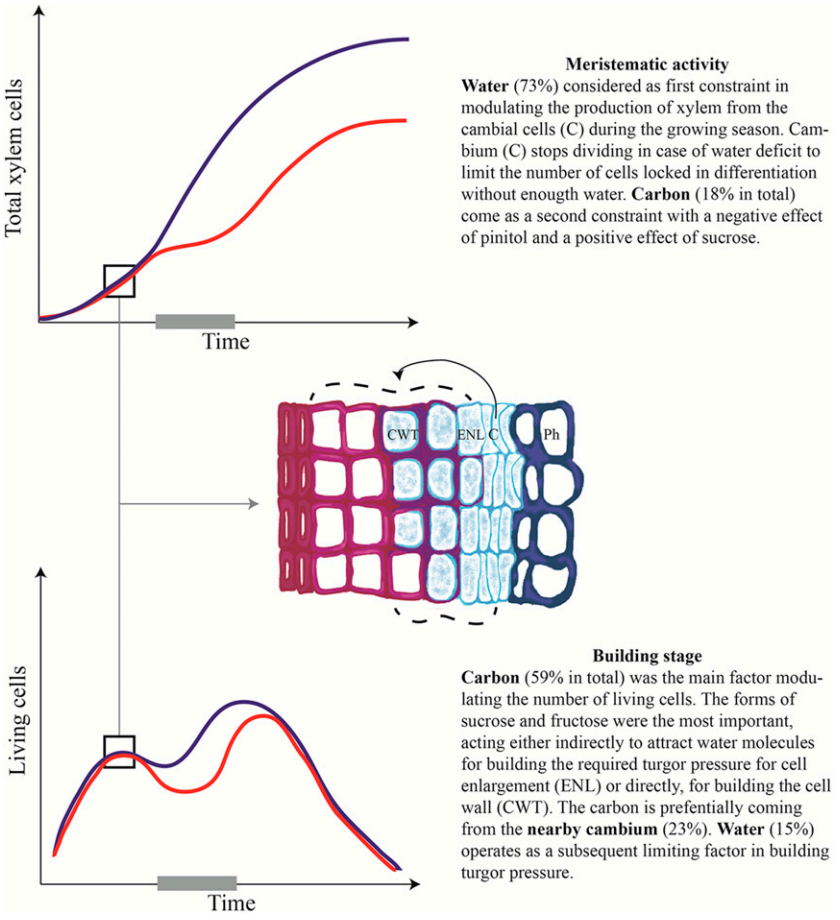

Figure 7. Illustration of the observed wood formation processes expressed as total xylem cells (top) and living cells (bottom) in the presence (red) and absence (blue) of water deficit (horizontal gray bars). A diagram of wood formation at the beginning of xylogenesis is shown to illustrate the measured processes. The implications of the DOV results are explained to stress the contributions of the factors in wood formation (for full explanation, see "Discussion"). Ph, Living phloem.

(i.e. raffinose) when the water potential drops (Deslauriers et al., 2014). Raffinose increases drastically during water deficit because this sugar acts mainly as an osmoprotector and a ROS scavenger (Nishizawa-Yokoi et al., 2008; dos Santos et al., 2011). The negative effect of this sugar on the living cells (Fig. 4, bottom), therefore, is perfectly in line with its main role.

The Role of Tissue in Supplying NSCs

Our mixed-effects model showed that NSCs extracted from cambium tissue were more important as a source of NSCs to predict the amount of living cells (DOV of 22.61%), as shown by the higher variance explained by cambium (Table III). However, the variable tissue was not significant in explaining the variation in total xylem cells, possibly because nonliving cells were included to account for the tree-ring increase over the growing season. Compared with the outermost xylem, much higher amounts of NSCs are found in cambium (Deslauriers et al., 2009; Simard et al., 2013), because of its proximity to the unloading sites in phloem. The recently produced NSCs are thus preferred in terms of C allocation (Carbone et al., 2013; Steppe et al., 2015), as phloem transport relies on the turgor pressure gradient created by the difference between sugar-loading and -unloading processes (De Schepper et al., 2013), represented here by the breakdown of sugars by the living cells (Figs. 1 and 7). The bimodal pattern in the number of living cells characterized by a slight depression in June is in agreement with previous observations in conifer species (Rossi et al., 2009), which were supposed to be associated with the internal competition for carbohydrates among meristems and the allocation priority toward primary growth. This hypothesis is confirmed by the reduction in Suc measured in cambium, especially in 2010, at the time of apical growth (DOY 160). In cambium, NSCs also can come from the hydrolysis of maltose during the process of starch degradation in bark at the beginning of the growing season (Oribe et al., 2003; Begum et al., 2013). Hence, our mixed-model results are in line with CASSIA dynamic growth model results, suggesting that cambial growth was sensitive to current-year C production (Schiestl-Aalto et al., 2015).

Girdling experiments, blocking the phloem translocation of photosynthates, also have demonstrated the foremost importance of current photoassimilate flux to sustain stem growth (Daudet et al., 2005). While some girdling studies indicated that NSC reserves in the stem were not sufficient to sustain growth below the girdle in the short term or the long term (de Schepper et al., 2010; Maier et al., 2010), others demonstrated that stem reserves could be used to restart growth (Daudet et al.,

2005; Maunoury-Danger et al., 2010). This assumption imposes source-sink relationships between xylem ray parenchyma cells and living cells (Olano et al., 2013). In the stem, ray parenchyma cells are the connective tissues between the different compartments (from the phloem to heartwood) and have many roles, such as reserve storage (Gartner et al., 2000) and respiration (Hou, 1985; Spicer and Holbrook, 2007). This could explain why less variance in the predicted living cells was represented by the NSCs extracted from the xylem tissues, even during drought. C storage indeed has priority over growth, reflecting a safety strategy in trees growing in cold or dry conditions. Hence, our result demonstrates that water is much more limiting than inner soluble sugars, in agreement with Palacio et al. (2014).

Effect of Water Deficit and Warming

The water deficit had a significant effect on both models, with a higher percentage of DOV on total cells (73%) compared with living cells (15%). Fewer tracheids were produced at the end of and after the period of water deficit. This was reflected first by the smaller populations of living cells and second by a temporary plateau in the total number of cells (Fig. 2). The mixed-model results show that water availability was ranked as the most significant factor explaining total xylem cell production, before any C factors (Fig. 6). This modulation of growth under low water is crucial to limit the number of living cells undertaking differentiation, which need water to fully complete their development. Otherwise, many differentiating cells would be locked in enlargement, without enough water to generate the suitable wall-yielding turgor pressure required for cell growth (Steppe et al., 2015). This key result confirms that radial growth, expressed here as the number of cells produced, is not source limited (Körner, 2003; Rocha, 2013; Palacio et al., 2014), because cambium is inhibited at a lower level of water stress than photosynthesis (Muller et al., 2011; Balducci et al., 2013; Fatichi et al., 2014). Similar conclusions were obtained with the CASSIA dynamic growth model (Schiestl-Aalto et al., 2015). For the living cells, however, water availability was ranked in the fifth position after C (Suc, Fru, and raffinose) and tissue (cambium). The apparent contradiction between these results could be explained by the low number of cambial cells with respect to differentiating cells, especially wall-thickening cells, and by the sugar compounds needed to build and maintain the turgor pressure of enlarging cells (Pantin et al., 2013; Steppe et al., 2015). In other words, once temperature and water availability are sufficient for cambial cells to divide, sugar compounds are allocated to start expansion (i.e. attracting water molecules) and, afterward, to thickening the cell walls.

The variance explained in both total xylem and living cells (as shown by the marginal r^2 when tissue and temperature treatment were fixed) decreased under water deficit, showing some uncoupling between NSCs and growth, especially for the living cells. This reduction could represent an alteration of NSC dependence on growth, caused by the reduced water availability (Muller et al., 2011), for three reasons. (1) Because wood formation practically stopped during water deficit, NSCs could be less required for wood formation processes (i.e. sink limitation), which, in turn, could reduce the variance explained. (2) In response to water deficit, the flow of available C, especially in the form of Suc, could be further directed to osmoregulation (i.e. forming raffinose) at the expense of growth. Although the quantities are minor, these carbohydrates are unavailable for osmotic purposes when sequestered in cell structures (cell wall and vacuoles; Pantin et al., 2013). (3) The accessibility and utilization of NSCs during water deficit is questioned (Sevanto et al., 2014), because the movement of NSCs decreases under low water content (Woodruff and Meinzer, 2011) and the translocation of carbohydrates in phloem becomes more limited under water stress (Woodruff, 2014).

The contribution of temperature in explaining total xylem cells was nonsignificant, while only T+2 was significant in explaining the number of living cells (2.63%), showing a marginal effect of temperature in our experiment. Although temperature is important in determining the potential growth rate (Pantin et al., 2012), little difference was found in wood formation (Balducci et al., 2013), possibly because the onset of growth was similar between treatments and the temperatures were well above the threshold limit for growth (Rossi et al., 2008) due to the greenhouse conditions. Lower amounts of hexose (Deslauriers et al., 2014) and starch in the ray parenchyma cells (Balducci et al., 2013) were measured under warmer growth temperatures, confirming the results of Way and Sage (2008) in black spruce trees. Although acclimation occurs, the increase in respiratory rate at higher temperature (Atkin and Tjoelker, 2003; Turnbull et al., 2004) may reduce the hexose pool in cambium and xylem. Even if this suggests a lower C availability for growth (particularly for cell enlargement), more studies are needed to characterize the role of temperature, especially under natural conditions.

CONCLUSION

Our analyses provide, to our knowledge for the first time, quantitative relationships linking NSCs and xylem development and including the influence of the nearby supply of C, water availability, and temperature. The mixed model elaborated in this study confirmed earlier observations about the parallel variation of sugars and differentiating xylem cells and is in line with the dynamic growth model. These results have important implications at the large ecological scale because cambial activity is responsible for the permanent sequestration of C in woody tissues (Cuny et al., 2015). The understanding of how C and water availability influence secondary growth is fundamental to improve growth models (Fatichi et al., 2014), and in this sense, we provide empirical knowledge

on important C compartments, xylem and cambium, and their respective roles in structural growth, including meristematic activity and tissue formation. However, our investigation was based on black spruce saplings, which might have different dynamics in terms of C requirements and allocation compared with older trees or trees of other species, especially if deciduous. Despite the fact that the mechanisms of xylem growth remain the same across ontogenetic states and species, caution in generalization of the results of this study for all trees must be taken due to potential variations in the timings and rates of C source (photosynthesis) and sink (wood formation).

MATERIALS AND METHODS

Experimental Design

The experiment was performed in a greenhouse complex located in Chicoutimi, Quebec, Canada (48°25′N, 71°04′W, 150 m above sea level) equipped with an automatic warming and cooling system that controls the environmental parameters. Four-year-old black spruce (*Picea mariana*) trees were transplanted into 4.5-L plastic pots with a peat moss, perlite, and vermiculite mix and left in an open field during a growing season and the following winter. In April 2010 and 2011, the saplings were taken into three different sections of the greenhouse for the experiment and fertilized with 1 g L^{-1} nitrogen:phosphorus:potassium (20:20:20) dissolved in 500 mL of water (Balducci et al., 2013). Three hundred saplings were installed in every section in both years, with a buffer zone of one additional row of saplings at the borders. Saplings were 48.9 ± 4.7 cm tall with a diameter of 8 ± 2 mm at the root collar and were provided with drip trickles for irrigation.

In one section of the greenhouse, the temperature was set to mimic the current thermal conditions of the region (T+0). Therefore, it was maintained as close as possible to the external air temperature, except on DOY 142 to 152 in 2010, when a technical problem occurred. The two other sections were subjected to specific thermal regimes (Fig. 2). In 2010, the treatments (called T+2 and T+5) consisted of a temperature 2 K and 5 K higher than T+0, respectively (Balducci et al., 2013). In 2011, the treatments (called T+6 daytime and T+6 nighttime) were 6 K warmer than T0 during the day (T+6 daytime; from 7 AM to 7 PM) or during the night (T+6 nighttime; from 7 PM to 7 AM; Fig. 2).

Two irrigation treatments were applied: (1) irrigated, consisting of maintaining the soil water content at approximately 80% of field capacity; and (2) water deficit, in which irrigation was withheld from mid-May to mid-June, the period when cambium is vigorously dividing (Rossi et al., 2006b). At the end of the water deficit period, the volumetric soil water content of nonirrigated saplings was less than 10%, while that of irrigated saplings varied between 40% and 50%. The predawn leaf water potential (Ψpd) of irrigated saplings was maintained close to −0.5 MPa in both years. During the water deficit, Ψ_{pd} of nonirrigated saplings dropped in response to the decrease of soil water availability, reaching the lowest values on DOY 172 (−2.7 ± 0.2 MPa) and DOY 180 (−1.3 ± 0.7 MPa) in 2010 and 2011, respectively. One week after the resumption of irrigation, the Ψ_{pd} of irrigated and nonirrigated saplings were similar, showing that the saplings were able to recover an optimal water status after the stress (Balducci et al., 2013; Deslauriers et al., 2014).

Xylem Growth

From May to September, 2010 and 2011, stem discs were collected weekly at 2 cm from the root collar of 36 randomly selected saplings (six saplings × two water regimes × three thermal treatments). At the same time, the apical growth (mm) was measured on each sapling with a precision digital caliber to the nearest 1 mm. The collected stem discs were dehydrated with successive immersions in ethanol and D-limonene, embedded in paraffin, and transverse sections of 8- to 10-μm thickness were cut with a rotary microtome (Rossi et al., 2006a).

The sections were stained with Cresyl Violet acetate (0.16% in water) and examined within 10 to 25 min with visible and polarized light at magnifications of 400× to 500× to distinguish the developing xylem cells. For each section, (1) cambial, (2) enlarging, (3) cell wall thickening, and (4) mature cells were counted along three radial files. In cross section, cambial cells were characterized by thin cell walls and small radial diameters. During cell enlargement, the tracheids still showed thin primary walls but radial diameters were at least twice those of the cambial cells. Observations under polarized light discriminated between enlarging and cell wall thickening tracheids. Because of the arrangement of the cellulose microfibrils, the developing secondary walls glistened when observed under polarized light, whereas no glistening was observed in enlargement zones, where the cells were still just composed of primary wall (Deslauriers et al., 2003). The progress of cell wall lignification was detected with Cresyl Violet acetate that reacts with the lignin (Rossi et al., 2006a). Lignification appeared as a color change from violet to blue. A homogenous blue color over the whole cell wall revealed the end of lignification and the reaching of tracheid maturity (Gričar et al., 2005).

NSC Extraction and Assessment

Every 2 weeks, 18 of the 36 saplings used for xylem analysis were selected for NSC assessment (three saplings × two water regimes × three thermal treatments). The branches were removed and the bark was separated from the wood to expose the cambial zone of the stem. The two parts (bark and wood) were plunged into liquid nitrogen and stored at −20°C. Dehydration was performed with a 5-d lyophilization. The cambium zone, probably including some cells in enlargement, was separated manually by scraping the inner part of the bark and the outermost part of the xylem with a surgical scalpel (Giovannelli et al., 2011). After having removed the cambium, the wood was milled to obtain a fine powder.

Soluble carbohydrate extraction followed the protocol of Giovannelli et al. (2011). For the cambium, only 1 to 30 mg of powder was available and used for the sugar extraction, while 30 to 600 mg of powder was available for wood. Samples with less than 1 mg of cambium powder were not considered, this quantity being lower than the HPLC detection limit. Soluble carbohydrates were extracted three times at room temperature with 5 mL of 75% ethanol added to the powder. A 100-μL volume of sorbitol solution (0.01 g mL^{-1}) also was added at the first extraction as an internal standard. In each extraction, the homogenates were vortexed gently for 30 min and centrifuged at 10,000 rpm for 8 min. The three resulting supernatants were evaporated and recuperated with 12 mL of nanofiltered water. This solution was then filtered by the solid-phase extraction method using a suction chamber with one column of N+ quaternary amino (200 mg 3 mL^{-1}) and one of CH (200 mg 3 mL^{-1}). The solution was evaporated to 1.5 mL and filtered through a 0.45-μm syringe filter into a 2-mL amber vial.

An Agilent 1200 series HPLC device with an refractive index detector and a Shodex SC 1011 column and guard column, equipped with an Agilent Chemstation for LC systems program, was used for soluble carbohydrate assessment. Calculations were made following the internal standard method described by Harris (1997). A calibration curve was created for each carbohydrate using pure Suc, raffinose, Glc, Fru (Canadian Life Science), and D-pinitol (Sigma-Aldrich). All fitting curves had r^2 of 0.99 and F values close to 1, indicating that each sugar had a 1:1 ratio with sorbitol. The quantity of sugar loss during extraction was calculated by comparing the concentrations of sorbitol added at the beginning of the extraction with those of unmanipulated sorbitol. The loss percentages were then calculated and added to the final results (Deslauriers et al., 2014).

Statistical Analysis

A mixed-effects model was used to fit the hierarchical data, in which an autocorrelation error structure in the repeated measurements over time was extended to level 1 that was nested within the measurements of different NSC concentrations (level 2) extracted from different tissues (level 3; Fig. 1) of the randomly selected trees (level 4). The trees were nested under different temperature treatments (level 5) and water treatments (level 6). In addition, there was a nested error structure (i.e. correlation among trees within temperature and water treatments). The mixed-effects model can deal effectively with this nested error structure to account for correlations associated with clustered data. Mixed-effects model techniques estimate fixed and random parameters simultaneously and give unbiased and efficient estimates of fixed parameters (Pinheiro and Bates, 2000).

Prior to the modeling analysis, the normality was checked and the square root of data transformation was then applied to the number of living cells and total xylem cells to meet the assumption of normality. Note that hereafter, the transformed data were used in the mixed-effects model analysis. Variance inflation factors (VIFs; Belsley et al., 1980) also were calculated to detect multicollinearity among the predictors, including Suc, D-pinitol, Glc, Fru, and raffinose.

VIFs were generally lower than the accepted value of 4 (O'Brien, 2007), except for Fru, which had a VIF greater than 10 due to collinearity with Glc, so it was removed from the model. Fru was kept, as this sugar is the product of both Suc synthase and invertase.

Fixed effects included different NSC concentrations (raffinose, Suc, D-pinitol, and Fru), measured tissue (xylem and cambium), temperatures (control T+0 versus T+2, T+5, T+6 daytime, and T+6 nighttime), water availability (water deficit and irrigated), and the interaction temperature × water. Random effects included trees and repeated measurements over time. In order to verify the two hypotheses, a mixed-effects model was built starting from a null model and then gradually extended to the higher levels (Singer, 1998). Therefore, a mathematical function can theoretically be expressed by both fixed and random effects as follows:

$$Y_{i(jklmt)} = \beta_0 + (\beta_1 + \mu_{1k})R_{i(jklmt)} + (\beta_2 + \mu_{2k})S_{i(jklmt)} + (\beta_3 + \mu_{3k})P_{i(jklmt)} + (\beta_4 + \mu_{4k})F_{i(jklmt)} + \beta_5 O_{jklm} + \beta_6 T_{lm} + \beta_7 W_m + \beta_8 T_{l(m)} W_m + \mu_{0k} + \varepsilon_{i(jklmt)}$$

where $Y_{i(jklmt)}$ is the ith (i = 1–3) measured cell number from the jth tissue (j = 0 and 1, indicating xylem and cambium, respectively) in the kth tree (k = 1–12) under the lth temperature treatment (l = 0 to 4, indicating T+0 versus T+2, T+5, T+6 daytime, and T+6 nighttime, respectively) and the mth water availability (m = 0 and 1, indicating water deficit and irrigated, respectively) on day t; β_0 is the overall mean; β_1 to β_8 are the corresponding fitted parameters; $R_{i(jklmt)}$, $S_{i(jklmt)}$, $P_{i(jklmt)}$, and $F_{i(jklmt)}$ are the ith measured NSC concentrations (raffinose, Suc, D-pinitol, and Fru, respectively) from the jth tissue in the kth tree under the lth temperature treatment and the mth water treatment on day t.

$T_{l(m)} \times W_m$ is the temperature × water interactive effects; μ_0 is a random intercept, and μ_1, μ_2, μ_3, and μ_4 are random slopes, where

$$\begin{pmatrix} \mu_0 \\ \mu_1 \\ \mu_2 \\ \mu_3 \\ \mu_4 \end{pmatrix} \sim N\left[\begin{pmatrix} 0 \\ 0 \end{pmatrix}, \begin{pmatrix} \tau_{00} & \tau_{01} \\ \tau_{10} & \tau_{11} \end{pmatrix}\right]$$

where τ_{00} and τ_{11} are the elements representing the variance components for the intercept and slope, respectively; τ_{10} is the covariance component representing correlation between the intercept and slope.

$\varepsilon_{i(jklmt)}$ is the random error associated with the ith measurements from the jth tissue of the kth tree under the lth temperature treatment and the mth water treatment on day t. $\varepsilon_{i(jklmt)} \sim N(0, \sigma_\varepsilon^2 \Omega)$, where

$$\sigma_\varepsilon^2 \Omega = \frac{\sigma_\varepsilon^2}{(1-\rho^2)} \begin{bmatrix} 1 & \rho & \rho^2 & \dots & \rho^{n-1} \\ \rho & 1 & \rho & \dots & \rho^{n-2} \\ \rho^2 & \rho & 1 & \dots & \rho^{n-3} \\ . & . & . & \dots & . \\ \rho^{n-1} & \rho^{n-2} & \rho^{n-3} & \dots & 1 \end{bmatrix}$$

and ρ is the autocorrelation coefficient, $|\rho| < 1$.

The mixed-effects model was built according to the conventional building process (Singer, 1998); the detailed mathematical and statistical approaches used have been described (Huang et al., 2014). A marginal r^2, which was calculated on the fixed effects only, and a conditional r^2, which was calculated on both fixed and random effects (Nakagawa and Schielzeth, 2013), also are provided to assess the overall performance of a mixed-effects model.

$$R^2_{marginal} = \frac{\delta_f^2}{\delta_f^2 + \delta_{tree}^2 + \delta_{ar(1)}^2 + \delta_\varepsilon^2 + 0.25}$$

$$R^2_{conditional} = \frac{\delta_f^2 + \delta_{tree}^2 + \delta_{ar(1)}^2}{\delta_f^2 + \delta_{tree}^2 + \delta_{ar(1)}^2 + \delta_\varepsilon^2 + 0.25}$$

where δ_f^2 is the variance calculated from the fixed-effect components of the mixed model and was estimated by multiplying the design matrix of the fitted effects with the vector of fixed-effects estimates (i.e. predicting fitted values based on fixed effects alone) followed by calculating the variance of these fitted values, δ^2_{tree} is the variance at tree level, $\delta^2_{ar(1)}$ is the variance for the first-order autocorrelation term, δ^2_ε is the variance for the error term, and 0.25 is the distribution-specific variance linked by square root.

To provide information regarding the variance explained at each level, the proportion change in variance (PCV) was calculated according to Merlo et al. (2005):

$$PCV_{tree} = 1 - \frac{\delta^2_{tree}}{\delta^2_{tree(null)}}$$

$$PCV_{ar(1)} = 1 - \frac{\delta^2_{ar(1)}}{\delta^2_{ar(1)(null)}}$$

$$PCV_{residual} = 1 - \frac{\delta^2_{residual}}{\delta^2_{residual(null)}}$$

where $\delta^2_{tree(null)}$, $\delta^2_{ar(1)(null)}$, and $\delta^2_{residual(null)}$ are the variances from the null model, respectively, and δ^2_{tree}, $\delta^2_{ar(1)}$, and $\delta^2_{residual}$ are the variances from the full model, respectively.

The assumption of normality of the residuals also was verified. In addition, the DOV (Huang et al., 2013, 2014) was determined to further quantify how much variance in the predicted square root of total xylem and living cells can be attributed to different fixed-effects predictors using SAS Proc GLM (type III). All analyses were conducted with SAS (version 9.3; SAS Institute).

ACKNOWLEDGMENTS

We thank Jacques Allaire, Daniel Gagnon, and Caroline Soucy for technical support and Alison Garside for checking the English text.

Received September 29, 2015; accepted February 2, 2016; published February 5, 2016.

LITERATURE CITED

Atkin OK, Tjoelker MG (2003) Thermal acclimation and the dynamic response of plant respiration to temperature. Trends Plant Sci **8:** 343–351

Balducci L, Deslauriers A, Giovannelli A, Rossi S, Rathgeber CBK (2013) Effects of temperature and water deficit on cambial activity and woody ring features in Picea mariana saplings. Tree Physiol **33:** 1006–1017

Begum S, Nakaba S, Yamagishi Y, Oribe Y, Funada R (2013) Regulation of cambial activity in relation to environmental conditions: understanding the role of temperature in wood formation of trees. Physiol Plant **147:** 46–54

Belsley D, Kuh E, Welsch R (1980) Regression Diagnostics: Identifying Influential Data and Sources of Collinearity. John Wiley & Sons, New York

Carbone MS, Czimczik CI, Keenan TF, Murakami PF, Pederson N, Schaberg PG, Xu X, Richardson AD (2013) Age, allocation and availability of nonstructural carbon in mature red maple trees. New Phytol **200:** 1145–1155

Cuny HE, Rathgeber CBK, Frank D, Fonti P, Fournier M (2014) Kinetics of tracheid development explain conifer tree-ring structure. New Phytol **203:** 1231–1241

Cuny HE, Rathgeber CBK, Frank D, Fonti P, Mäkinen H, Prislan P, Rossi S, del Castillo EM, Campelo P, et al (2015) Intra-annual dynamics of woody biomass production in coniferous forests. Nature Plants **1:** 15160

Daudet FA, Améglio T, Cochard H, Archilla O, Lacointe A (2005) Experimental analysis of the role of water and carbon in tree stem diameter variations. J Exp Bot **56:** 135–144

De Schepper V, De Swaef T, Bauweraerts I, Steppe K (2013) Phloem transport: a review of mechanisms and controls. J Exp Bot **64:** 4839–4850

de Schepper V, Steppe K, Van Labeke MC, Lemeur R (2010) Detailed analysis of double girdling effects on stem diameter variations and sap flow in young oak trees. Environ Exp Bot **68:** 149–156

Deslauriers A, Beaulieu M, Balducci L, Giovannelli A, Gagnon MJ, Rossi S (2014) Impact of warming and drought on carbon balance related to wood formation in black spruce. Ann Bot (Lond) **114:** 335–345

Deslauriers A, Giovannelli A, Rossi S, Castro G, Fragnelli G, Traversi L (2009) Intra-annual cambial activity and carbon availability in stem of poplar. Tree Physiol **29:** 1223–1235

Deslauriers A, Morin H, Begin Y (2003) Cellular phenology of annual ring formation of *Abies balsamea* in Quebec boreal forest (Canada). Can J For Res **33:** 190–200

dos Santos TB, Budzinski IGF, Marur CJ, Petkowicz CLO, Pereira LFP, Vieira LGE (2011) Expression of three galactinol synthase isoforms in Coffea arabica L. and accumulation of raffinose and stachyose in response to abiotic stresses. Plant Physiol Biochem **49:** 441–448

Fatichi S, Leuzinger S, Körner C (2014) Moving beyond photosynthesis: from carbon source to sink-driven vegetation modeling. New Phytol **201:** 1086–1095

Freixes S, Thibaud MC, Tardieu F, Muller B (2002) Root elongation and branching is related to local hexose concentration in Arabidopsis thaliana seedlings. Plant Cell Environ **25:** 1357–1366

Gartner B, Baker D, Spicer R (2000) Distribution and vitality of xylem rays in relation to leaf area in Douglas-fir. IAWA J **21:** 389–401

Giovannelli A, Emiliani G, Traversi ML, Deslauriers A, Rossi S (2011) Sampling cambial region and mature xylem for non structural carbohydrates and starch analyses. Dendrochronologia **29:** 177–182

Gričar J, Čufar K, Oven P, Schmitt U (2005) Differentiation of terminal latewood tracheids in silver fir trees during autumn. Ann Bot (Lond) **95:** 959–965

Gruber A, Strobl S, Veit B, Oberhuber W (2010) Impact of drought on the temporal dynamics of wood formation in Pinus sylvestris. Tree Physiol **30:** 490–501

Gruber A, Wieser G, Oberhuber W (2009) Intra-annual dynamics of stem CO_2 efflux in relation to cambial activity and xylem development in Pinus cembra. Tree Physiol **29:** 641–649

Hansen J, Beck E (1990) The fate and path of assimilation products in the stem of 8-year-old Scots pine (*Pinus sylvestris* L.) trees. Trees Struct Funct **4:** 16–21

Hansen J, Beck E (1994) Seasonal change in the utilization and turnover of assimilation products in 8-year-old Scots pine (*Pinus sylvestris* L.) trees. Trees Struct Funct **8:** 172–182

Harris DC (1997) Internal standards. *In* Quantitative Chemical Analysis, Ed 5. WH Freeman, New York, p 104

Hou W (1985) Seasonal fluctuation of reserve materials in the trunkwood of spruce [*Picea abies* (L.) Karst.]. J Plant Physiol **117:** 355–362

Huang JG, Bergeron Y, Berninger F, Zhai L, Tardif JC, Denneler B (2013) Impact of future climate on radial growth of four major boreal tree species in the eastern Canadian boreal forest. PLoS ONE **8:** e56758

Huang JG, Deslauriers A, Rossi S (2014) Xylem formation can be modeled statistically as a function of primary growth and cambium activity. New Phytol **203:** 831–841

Johnson JM, Pritchard J, Gorham J, Tomos AD (1996) Growth, water relations and solute accumulation in osmotically stressed seedlings of the tropical tree *Colophospermum mopane*. Tree Physiol **16:** 713–718

Kagawa A, Sugimoto A, Maximov TC (2006) $^{13}CO_2$ pulse-labelling of photoassimilates reveals carbon allocation within and between tree rings. Plant Cell Environ **29:** 1571–1584

Koch K (2004) Sucrose metabolism: regulatory mechanisms and pivotal roles in sugar sensing and plant development. Curr Opin Plant Biol **7:** 235–246

Körner C (2003) Carbon limitation in trees. J Ecol **91:** 4–17

Lastdrager J, Hanson J, Smeekens S (2014) Sugar signals and the control of plant growth and development. J Exp Bot **65:** 799–807

Lavigne MB, Little CHA, Riding RT (2004) Changes in stem respiration rate during cambial reactivation can be used to refine estimates of growth and maintenance respiration. New Phytol **162:** 81–93

Maier CA, Johnsen KH, Clinton BD, Ludovici KH (2010) Relationships between stem CO_2 efflux, substrate supply, and growth in young loblolly pine trees. New Phytol **185:** 502–513

Maunoury-Danger F, Fresneau C, Eglin T, Berveiller D, François C, Lelarge-Trouverie C, Damesin C (2010) Impact of carbohydrate supply on stem growth, wood and respired CO_2 $\delta^{13}C$: assessment by experimental girdling. Tree Physiol **30:** 818–830

Merlo J, Chaix B, Yang M, Lynch J, Råstam L (2005) A brief conceptual tutorial on multilevel analysis in social epidemiology: interpreting neighbourhood differences and the effect of neighbourhood characteristics on individual health. J Epidemiol Community Health **59:** 1022–1028

Michelot A, Simard S, Rathgeber C, Dufrêne E, Damesin C (2012) Comparing the intra-annual wood formation of three European species (Fagus sylvatica, Quercus petraea and Pinus sylvestris) as related to leaf phenology and non-structural carbohydrate dynamics. Tree Physiol **32:** 1033–1045

Muller B, Pantin F, Génard M, Turc O, Freixes S, Piques M, Gibon Y (2011) Water deficits uncouple growth from photosynthesis, increase C content, and modify the relationships between C and growth in sink organs. J Exp Bot **62:** 1715–1729

Nakagawa S, Schielzeth H (2013) A general and simple method for obtaining r^2 from generalized linear mixed-effects models. Methods Ecol Evol **4:** 133–142

Nishizawa-Yokoi A, Yabuta Y, Shigeoka S (2008) The contribution of carbohydrates including raffinose family oligosaccharides and sugar alcohols to protection of plant cells from oxidative damage. Plant Signal Behav **3:** 1016–1018

O'Brien R (2007) A caution regarding rules of thumb for variance inflation factors. Qual Quant **41:** 673–690

Olano JM, Arzac A, García-Cervigón AI, von Arx G, Rozas V (2013) New star on the stage: amount of ray parenchyma in tree rings shows a link to climate. New Phytol **198:** 486–495

Oribe Y, Funada R, Kubo T (2003) Relationships between cambial activity, cell differentiation and the localization of starch in storage tissues around the cambium in locally heated stem of *Abies sachalinensis* (Schmidt) Master. Trees Struct Funct **14:** 185–192

Orthen B, Popp M, Smirnoff N (1994) Hydroxyl radical scavenging properties of cyclitols. Proc R Soc Edinb [Biol] **102:** 269–272

Palacio S, Hoch G, Sala A, Körner C, Millard P (2014) Does carbon storage limit tree growth? New Phytol **201:** 1096–1100

Pantin F, Fanciullino AL, Massonnet C, Dauzat M, Simonneau T, Muller B (2013) Buffering growth variations against water deficits through timely carbon usage. Front Plant Sci **4:** 483

Pantin F, Simonneau T, Muller B (2012) Coming of leaf age: control of growth by hydraulics and metabolics during leaf ontogeny. New Phytol **196:** 349–366

Pinheiro J, Bates D (2000) Mixed-Effects Models in S and S-PLUS. Springer, New York

Rocha AV (2013) Tracking carbon within the trees. New Phytol **197:** 685–686

Rossi S, Anfodillo T, Cufar K, Cuny HE, Deslauriers A, Fonti P, Frank D, Gricar J, Gruber A, King GM, et al (2013) A meta-analysis of cambium phenology and growth: linear and non-linear patterns in conifers of the northern hemisphere. Ann Bot (Lond) **112:** 1911–1920

Rossi S, Anfodillo T, Menardi R (2006a) Trephor: a new tool for sampling microcores from tree stems. IAWA J **27:** 89–97

Rossi S, Deslauriers A, Anfodillo T, Morin H, Saracino A, Motta R, Borghetti M (2006b) Conifers in cold environments synchronize maximum growth rate of tree-ring formation with day length. New Phytol **170:** 301–310

Rossi S, Deslauriers A, Griçar J, Seo JW, Rathgeber CBK, Anfodillo T, Morin H, Levanic T, Oven P, Jalkanen R (2008) Critical temperatures for xylogenesis in conifers of cold climates. Glob Ecol Biogeogr **17:** 696–707

Rossi S, Simard S, Rathgeber C, Deslauriers A, De Zan C (2009) Effects of a 20-day-long dry period on cambial and apical meristem growth in *Abies balsamea* seedlings. Trees (Berl) **23:** 85–93

Scheible WR, Lauerer M, Schulze ED, Caboche M, Stitt M (1997) Accumulation of nitrate in the shoot acts as a signal to regulate shoot-root allocation in tobacco. Plant J **11:** 671–691

Schiestl-Aalto P, Kulmala L, Mäkinen H, Nikinmaa E, Mäkelä A (2015) CASSIA: a dynamic model for predicting intra-annual sink demand and interannual growth variation in Scots pine. New Phytol **206:** 647–659

Sevanto S, McDowell NG, Dickman LT, Pangle R, Pockman WT (2014) How do trees die? A test of the hydraulic failure and carbon starvation hypotheses. Plant Cell Environ **37:** 153–161

Simard S, Giovannelli A, Treydte K, Traversi ML, King GM, Frank D, Fonti P (2013) Intra-annual dynamics of non-structural carbohydrates in the cambium of mature conifer trees reflects radial growth demands. Tree Physiol **33:** 913–923

Singer J (1998) Using SAS Proc Mixed to fit multilevel models, hierarchical models, and individual growth models. J Educ Behav Stat **24:** 323–355

Spicer R, Holbrook NM (2007) Parenchyma cell respiration and survival in secondary xylem: does metabolic activity decline with cell age? Plant Cell Environ **30:** 934–943

Steppe K, Sterck F, Deslauriers A (2015) Diel growth dynamics in tree stems: linking anatomy and ecophysiology. Trends Plant Sci **20:** 335–343

Tardieu F, Granier C, Muller B (2011) Water deficit and growth: coordinating processes without an orchestrator? Curr Opin Plant Biol **14:** 283–289

Turnbull MH, Tissue DT, Murthy R, Wang XZ, Sparrow AD, Griffin KL (2004) Nocturnal warming increases photosynthesis at elevated CO_2 partial pressure in *Populus deltoides*. New Phytol **161:** 819–826

Way DA, Sage RF (2008) Elevated growth temperatures reduce the carbon gain of black spruce *Picea mariana* (Mill.) BSP. Glob Change Biol **14:** 624–636

Wiley E, Helliker B (2012) A re-evaluation of carbon storage in trees lends greater support for carbon limitation to growth. New Phytol **195:** 285–289

Woodruff DR (2014) The impacts of water stress on phloem transport in Douglas-fir trees. Tree Physiol **34:** 5–14

Woodruff DR, Meinzer FC (2011) Water stress, shoot growth and storage of non-structural carbohydrates along a tree height gradient in a tall conifer. Plant Cell Environ **34:** 1920–1930